Elsevier Editorial System(tm) for Membrane Science
Manuscript Draft

Manuscript Number: JMS-071039R1

Title: Thermodynamics of Pore Wetting and Swelling in Nafion

Article Type: Full Length Article

Keywords: Nafion; wetting; swelling; sorption; equilibrium

Corresponding Author: Mr. Gwynn Elfring,

Corresponding Author's Institution: University of Victoria

First Author: Gwynn J Elfring

Order of Authors: Gwynn J Elfring; Henning Struchtrup, Dr.-Ing

Abstract: A model for the wetting and swelling of pores with water within a Nafion membrane, based on minimizing all contributions to the total free energy, is developed. We find that equilibrium state depends on entropic mixing forces and energetic surface forces. The wetting of the pore relies on the entropic forces exceeding the energetic forces. If the pore fills with liquid it will swell until balanced by the energy of the deforming membrane. Several factors including pressure relative to saturation and the phase which bounds the membrane are shown to dramatically affect the final equilibrium state of the system.

Thermodynamics of Pore Wetting and Swelling in Nafion

Gwynn J. Elfring * Henning Struchtrup

Institute for Integrated Energy Systems, Department of Mechanical Engineering, University of Victoria PO Box 3055 STN CSC, Victoria BC V8W 3P6, Canada

Abstract

A model for the wetting and swelling of pores with water within a Nafion membrane, based on minimizing all contributions to the total free energy, is developed. We find that equilibrium state depends on entropic mixing forces and energetic surface forces. The wetting of the pore relies on the entropic forces exceeding the energetic forces. If the pore fills with liquid it will swell until balanced by the energy of the deforming membrane. Several factors including pressure relative to saturation and the phase which bounds the membrane are shown to dramatically affect the final equilibrium state of the system.

Key words: Nafion, Wetting, Swelling, Sorption, Equilibrium

1 Introduction

The transport through bulk water presents an upper limit for protonic conductivity; therefore, it is important to determine the permeation of the liquid phase and its connectivity in order to quantify the various modes of proton transport. Due to the complex nature of Nafion, SAS and WAXD studies reveal little morphological detail [1]; therefore, a number of descriptions of Nafion morphology which differ significantly in their proposed spatial distribution of ionic domains have been proposed.

In some of the earliest studies, Gierke et al. examined Nafion with small angle X-ray spectroscopy (SAXS) and wide-angle X-ray diffraction (WAXD) [2],

* Corresponding author.
Email address: gelfring@uvic.ca (Gwynn J. Elfring).

[3],[4]. From these studies they postulated the existence ionic clusters, 3-5 nm in diameter, which are spherical inverse micellar in structure. In order to explain the high ionic conductivity found in Nafion, Gierke et al. proposed these clusters were connected by channels, 1-2 nm in diameter, yielding a cluster network. A core-shell model was proposed by Fujimura, similar to the Gierke model, where an ion rich core is surrounded by an ion poor shell which are dispersed in a matrix of fluorocarbon chains [5], [6]. Another early model, by Yeager and Steck, proposed the existence of three distinct regions within the membrane: (A) a hydrophobic matrix, (B) an interfacial zone and, (C) ionic clusters [7]. They propose that the ionic clusters are regions within the membrane with a higher concentration of sulfonate acid sites at which the water will tend to agglomerate. Litt proposed that ionic domains are hydrophilic layers separated by thin lamellar PTFE crystallites [8]. Haubold et al. proposed a similar structure to that of Litt, where the side chains and sulfonate groups form shell layers which bound a core layer that can be either dry or filled with solvent, forming a 'sandwich' structure [9]. A local order model was introduced by Dreyfus et al. which is based on the existence of a short range order, long range gas-like disorder and a fixed number of neighboring ionic aggregates [10]. Kreuer provided an interpretation of SAXS data which is based on the idea of a random arrangement of low dimensional polymeric objects with spaces which can be filled by water [11]. Such a description is also reflected in the AFM imaging conducted by McLean et al.[12]. Recently the work of Schmidt-Rohr and Chen suggests a parallel cylindrical pore model best suits the features of SAXS data [13], despite the fact that such a model has not gained traction in the past amongst experimentalists [1]. This list is by no means complete but serves to show the discordant interpretations of experimental data that have been proposed. A far more exhaustive summary of morphological models is given by Mauritz [1].

In the present work, based on previous work in [14], we aim at adding analytical insight to the wealth of experimental work done in determining the morphology of Nafion. Previous work such as that done by Choi et al.[15] [16], and Futerko and Hsing [17], determine sorption in the membrane as a whole in order to quantify sorption isotherms. Here the focus is on sorption on the scale of micropores [18], in order to help quantify the complex microstructure of Nafion as it sorbs water, in particular the distribution and connectivity of the hydrophilic domain, and to add insight to the development of pore based transport models such as [19], [20], [21]. Previously, we formulated a total Gibbs free energy of a cylindrical pore system to determine whether or not liquid would wet the pore depending on geometry [14]. In this work we introduce spherical pores and construct 'cluster-network' configurations to observe the effect of coupling spherical and cylindrical pores on the stability of the liquid phase. We also introduce pore swelling and examine the effects of pore geometry on swelling.

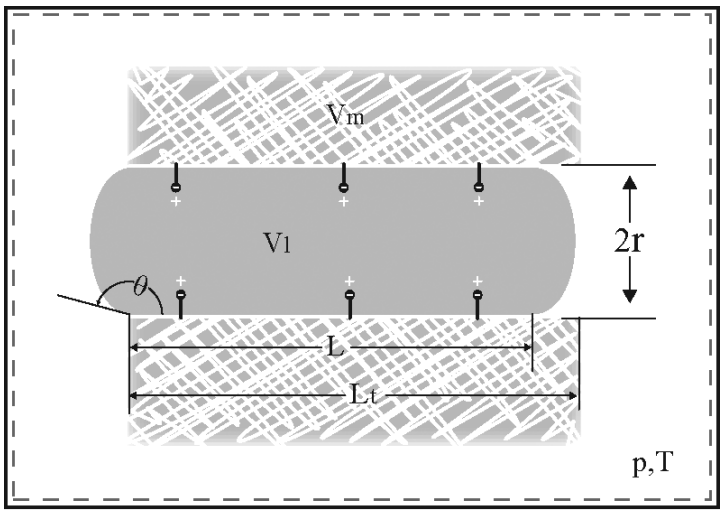

Fig. 1. Cylindrical Pore System [14]

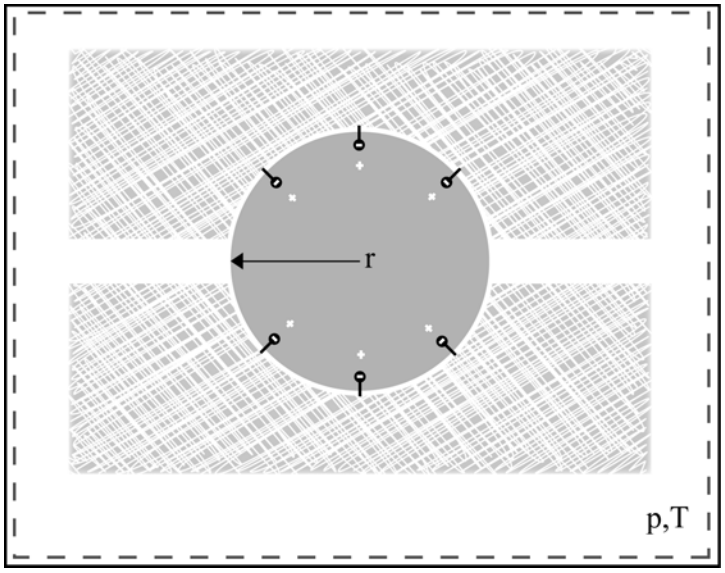

Fig. 2. Spherical Pore System

2 Total Gibbs Free Energy

The system we consider here is a closed system with a single Nafion pore subject to a fixed pressure p, and temperature T [14]. See Figure 1 for a cylindrical pore and Figure 2 for a spherical pore. The environment considered is at or near saturation and therefore the chemical reaction dissociating the sulfonate sites is considered to have occurred, whether or not bulk-like liquid fills the pore.

From the first and second laws of thermodynamics, for a system with fixed external pressure and temperature, one finds that the total Gibbs free energy

in a system, $\mathcal{G}$, goes to a minimum in equilibrium [22]:

$$\frac{d\mathcal{G}}{dt} \leq 0\,. \tag{1}$$

Writing out all contributions to $\mathcal{G}$ in terms of the Gibbs free energy in the unmixed state, $G_\alpha = g_\alpha(T,p)m_\alpha$, and the Gibbs free energy of mixing, $G_{\alpha,mix}$, gives

$$\mathcal{G} = G_l + G_{l,mix} + G_p + G_{p,mix} + G_v + G_s + G_m\,. \tag{2}$$

The subscripts $\alpha = l$, p, v, s, and m refer to the liquid, protons, vapor, surface and membrane, respectively. Since the membrane is phase-separated, there is no mixing of the polymer chains with the liquid in the pore and thus no corresponding entropic contributions.

Equation (2) is our governing equation in its most general form. This equation is transformed by taking vapor as an ideal gas, assuming the liquid water and protons in the mixture are incompressible, along with various constitutive relations and mathematical techniques outlined in detail in [14], into a function of geometric variables we are concerned with. We also introduce as a reference state, the total free energy of a vapor filled pore $\mathcal{G}^0$ and subtract this from Equation (2) to obtain

$$\begin{aligned}\mathcal{G} - \mathcal{G}^0 = &\left[(p - p_{sat}) + \frac{R_w T}{v_l}\ln\left(\frac{X_l}{p_r}\right)\right] V_l \\ &+ \left[g_p\left(p\right) - g_p^0\left(p\right) + R_p T\left(\ln\left(1 - X_l\right) + \chi_{pl}X_l\right)\right] m_p \\ &+ G_m - G_m^0 + G_s\ - G_s^0. \end{aligned}\tag{3}$$

Here, R_α denotes the gas constant, where $R_l = R_v = R_w$. The protons within the liquid mixture are referred to by m_p and V_p, while the protons outside the liquid boundary are denoted by m_p^0 and V_p^0; χ_{pl} is the Flory interaction parameter between liquid and proton [23]. The pressure relative to saturation is denoted as $p_r = p/p_{sat}$ and the mole fraction of the liquid water in the mixture is given by

$$X_l = \frac{N_l}{N_p + N_l} \tag{4}$$

where N_α is the mole number. The mole fraction of the protons in the mixture is $X_p = 1 - X_l$.

We are interested in determining whether liquid or vapor is energetically favorable in a given pore. By subtracting the free energy of a vapor filled pore, we know that if the difference $\mathcal{G} - \mathcal{G}^0$ is negative, then the free energy of the vapor state is lower and therefore the vapor filled state is stable in equilibrium. Subtraction of $\mathcal{G}^0$ also conveniently eliminates various constants if $r = r_0$, which

occurs when we do not consider membrane swelling. We still have unknown functions remaining in the free energy of the protons $g_p(p) - g_p^0(p)$, the free energy of the membrane $G_m - G_m^0$, and the surface free energy $G_s - G_s^0$. The subsequent sections detail revealing the structure of these functions.

2.1 Dissociation

Initially the $H^+(H_2O)_n$ is very strongly bound to the $-SO_3^-$ group where the proton originated. As more waters are attracted to this acid site, a fraction of the water is strongly bound in proton-transfer complexes [17]. This reduces the effective water content of the membrane, and in turn increases the mobility of the dissociated proton. It was proposed by Futerko et al. to treat the fraction of waters strongly bound to the acid site λ_C (akin to chemisorption) as part of the polymer, separate from the water that is free to equilibrate the chemical potential of the system λ_F [17]. Therefore the total number of waters per acid site in the membrane is given as $\lambda = \lambda_F + \lambda_C$. We assume that for the vapor filled reference state the dissociation reaction has taken place and λ_C water molecules are strongly bound to the sulfonate site. The number of these waters is evaluated through the law of mass action as described by Choi and Datta [15]. These waters are strongly bound and exist regardless of whether a liquid phase fills the pore. For the purpose of this work, we assume that the subsequent waters which form the liquid phase do not significantly alter the free energy of the protons, therefore the $g_p(p) - g_p^0(p)$ term is negligible and the bulk-like waters λ_F contribute in altering the total free energy due to mixing only.

2.2 Elastic Free Energy

A change in the free energy of the membrane due to elastic forces occurs when the membrane swells to a radius r greater than the initial radius r_0, in order to accommodate more liquid. The change in free energy of a polymer is entropic, when the material is stretched the polymer chains have their configurational entropy reduced. Flory developed a model which assumes a linear strain in the deformation of the chains comprising the network and a Gaussian distribution of polymer chain lengths [23]. Flory finds the change in free energy

$$G_m - G_m^0 = \frac{kT\nu_e}{2}\left[\alpha_1^2 + \alpha_2^2 + \alpha_3^2 - 3 - \ln(\alpha_1\alpha_2\alpha_3)\right] \tag{5}$$

where k is the Boltzmann constant and α_β is the linear deformation factor. ν_e is the elastically effective number of chains in the polymer network. Freger points out that for a phase-separated polymer network such as Nafion, the as-

sumption made in Flory-Rehner theory may not be appropriate; that neglecting the interaction of the aggregates upon swelling is too large a simplification [24]. Freger has developed an adaptation of the classical Flory-Rehner model which describes the phase-separated swelling of the hydrophobic matrix as an 'inflation' rather than a dilution. Freger [24] proposes, for isotropic swelling ($\alpha_\beta = \alpha$), the form

$$G_m - G_m^0 = \frac{kT\nu_e}{2V_0}\left[2\alpha^{-2/3} + \alpha^{4/3}\right]. \tag{6}$$

In the present analysis we use Flory's form. Flory's model is an oversimplification not only because of the nature of the phase separation and but also because there is both evidence of crystallinity which would cause effective cross-linking and evidence of anisotropy through elongated polymeric aggregates [25]. These factors are also not addressed by the Freger model, which is not used as it would give a finite elastic free energy in the undeformed state. A comprehensive description of the elastic deformation of Nafion has yet to be formulated; however, since we consider a single microscopic pore, the phase separation is already considered explicitly.

To define the number of chains that a pore is stretching we assume that the volume of membrane being swollen is linearly proportional to the volume of the pore

$$V_m^T = \frac{V_0}{\phi}. \tag{7}$$

Here V_m^T refers to the total membrane volume of a pore, which includes pore and backbone. The constant ϕ is a measure of the porosity of the membrane and V_0 refers to the volume of the unswollen pore in the membrane. What this means is that each pore stretches a region of the membrane which is proportional to its own volume. This divides the membrane in pores and the volume of membrane that bounds in a strategy similar to that employed by Freger. Therefore the number of chains stretched by one pore is assumed to be

$$\nu_e = \frac{V_0 A_v}{\phi \bar{V}_m^T}\ . \tag{8}$$

This strategy is used as a first estimate to establish the number of chains stretched during the deformation of a pore. In a subsequent section we vary this value to determine the impact of varying membrane thickness about a pore.

2.3 Surface Free Energy

The surface free energy is the additional free energy required to remove a molecule from the bulk in order to create an interface between two coexisting

phases [26]. This energy is linearly proportional to the surface area of the interface,

$$G_s = \gamma \int dA \,, \tag{9}$$

where γ is the interfacial tension which has units of energy per unit area. In our system we have three phase interfaces, and thus the surface free energy of the system is

$$G_s = \gamma_{sv} A_{sv} + \gamma_{sl} A_{sl} + \gamma_{lv} A_{lv} \tag{10}$$

where γ_{sv}, γ_{sl} and γ_{lv} are the interfacial tensions of the solid-vapor, solid-liquid and liquid-vapor interfaces, respectively [26]. The surface free energy of the reference state is given simply by

$$G_s^0 = \gamma_{sv} A_{sv}^0 \ . \tag{11}$$

Young's equation,

$$\frac{\gamma_{sv} - \gamma_{sl}}{\gamma_{lv}} = \cos\theta \,, \tag{12}$$

relates the surface tensions to the contact angle at the three phase point.

2.4 Geometry Depedant Form

We now have a form of the total Gibbs free energy 2, which depends only on geometric terms

$$\begin{aligned} \mathcal{G} - \mathcal{G}^0 = &\left[(p - p_{sat}) + \frac{R_w T}{v_l} \ln\left(\frac{X_l}{p_r}\right) \right] V_l \\ &+ R_u T \left[\ln(1 - X_l) + \chi_{pl} X_l \right] A_{sl}^U S_p + \frac{kT\nu_e}{2} \left[\alpha_1^2 + \alpha_2^2 + \alpha_3^2 - 3 - \ln(\alpha_1 \alpha_2 \alpha_3) \right] \\ &+ \gamma_{sv} \left(A_{sv} - A_{sv}^0 \right) + \gamma_{sl} A_{sl} + \gamma_{lv} A_{lv} \ . \end{aligned} \tag{13}$$

where S_p represents the surface density of sulfonate sites (which are assumed to be ionized) and A_{sl}^U is the surface area of the unswollen pore in contact with liquid. The mole fraction of liquid is then given by

$$X_l = \frac{V_l}{\beta A_{sl}^U + V_l} \tag{14}$$

where $\beta = S_p M_w / \rho_w$; M_w is the molar mass of water and ρ_w is the mass density of liquid water.

2.5 Spherical System

We now apply the spherical geometry into the equilibrium conditions. The pore is either filled with liquid completely or is empty, we do not consider a partially full pore with finite $r < r_0$. The spherical agglomeration of liquid water, which has a surface area of $A_l = 4\pi r^2$ and volume $V_l = \frac{4}{3}\pi r^3$, only has partial contact with the Nafion backbone such that the area of the solid-liquid interface $A_{sl} = nA_l = n4\pi r^2$. The surface area of the unswollen pore in contact with liquid is then $A_{sl}^U = n4\pi r_0^2$ when full. The area of the liquid-vapor interface, represented by the openings in Figure 2, is $A_{lv} = (1-n)\,A_l$ and $A_{sv} - A_{sv}^0 = -n\pi r_0^2$ where r_0 refers to the initial radius of the pore.

We assume that, when the membrane swells, the volume of the membrane backbone itself remains constant, $V_m = V_m^0$. For the swelling of a spherical pore the deformation along the surface of the pore is $\alpha_1 = r/r_0$ and $\alpha_2 = r/r_0$ and with $V_m = V_m^0$, then $\alpha_1\alpha_2\alpha_3 = 1$ therefore the change in thickness of the membrane is given by $\alpha_3 = (r_0/r)^2$. With this, along with equation (8), the elastic free energy of the membrane (5) then becomes

$$G_m - G_m^0 = \frac{2kT\pi r_0^3 L_t A_v}{3\phi \bar{V}_m^T}\left[2\left(\frac{r}{r_0}\right)^2 + \left(\frac{r_0}{r}\right)^4 - 3\right], \tag{15}$$

for a spherical pore.

With the aforementioned geometric formulations for a spherical geometry, (13) therefore yields,

$$\begin{aligned}\mathcal{G} - \mathcal{G}^0 = &\left[(p - p_{sat}) + \frac{R_w T}{v_l}\ln\left(\frac{r^3}{p_r\left[r^3 + 3\beta n r_0^2\right]}\right)\right]\frac{4}{3}\pi r^3 \\ &+ R_u T\left[\ln\left(1 - \frac{r^3}{r^3 + 3\beta n r_0^2}\right) + \frac{r^3}{r^3 + 3\beta n r_0^2}\chi_{pl}\right] S_p n 4\pi r_0^2 \\ &+ \frac{2kT\pi r_0^3 L_t A_v}{3\phi \bar{V}_m^T}\left[2\left(\frac{r}{r_0}\right)^2 + \left(\frac{r_0}{r}\right)^4 - 3\right] \\ &+ \gamma_{sv} n 4\pi(r^2 - r_0^2) + \gamma_{lv}(1 - n - n\cos\theta)4\pi r^2\,. \end{aligned} \tag{16}$$

Equation (16) is our governing equation for the spherical pore. It is entirely defined by the geometric parameters n, r and r_0 and the state variables p and T which are imposed on the system.

2.6 Cylindrical System

The geometry of the cylindrical pore is as shown in Figure 1. It is assumed that the liquid agglomeration fills the pore completely in the radial while the filling length L is varied or the pore is assumed empty. Situations in which the radius of the liquid r is smaller than the unswollen radius of the pore r_0 are not considered. The surface area of the liquid is $A_l = 2\pi rL + 2\pi r^2 a_\theta$ and the volume of the liquid is $V_l = \pi r^2 L + 2\frac{\pi}{3} r^3 b_\theta$ where $a_\theta = 2\left[1 + \sin\theta\right]^{-1}$ and $b_\theta = 2\sec^3\theta\left[\sin\theta - 1\right] + \tan\theta$ are functions which define the curvature of the ends. The area of solid-liquid interface $A_{sl} = 2\pi rL$, the liquid-vapor interface $A_{lv} = 2\pi r^2 a_\theta$ and $A_{sv} - A_{sv}^0 = 2\pi r(L_t - L)$, where L_t is the total length of the pore. The area of the unstretched solid-liquid interface $A_{sl}^U = 2\pi r_0 L_t$. When the length L of the liquid in the pore is zero, $V_l = 2V_{end}$, due to the curved ends which remain.

For the swelling of a cylindrical pore we constrain deformation of L_t such that $\alpha_1 = 1$. The stretching of the length of the perimeter of the cylinder is $\alpha_2 = r/r_0$. Because we assume $V_m = V_m^0$, then $\alpha_1\alpha_2\alpha_3 = 1$, and therefore the thickness of the membrane surrounding the pore changes by $\alpha_3 = 1/\alpha_2$. Substituting this into equation (5) yields

$$G_m - G_m^0 = \frac{kT\pi r_0^2 L_t A_v}{2\phi \bar{V}_m^T}\left[\left(\frac{r}{r_0}\right)^2 + \left(\frac{r_0}{r}\right)^2 - 2\right] \ . \tag{17}$$

With the geometric delineation given above for a cylindrical geometry, (13) therefore yields,

$$\begin{aligned}\mathcal{G} - \mathcal{G}^0 = &\left[(p - p_{sat}) + \frac{R_w T}{v_l}\ln\left(\frac{r^2L + 2r^3 b_\theta}{p_r\left[2\beta r_0 L + r^2 L + 2r^3 b_\theta\right]}\right)\right]\left(\pi r^2 L + \frac{2\pi r^3}{3} b_\theta\right) \\ &+ R_u T\left[\ln\left(1 - \frac{r^2L + 2r^3 b_\theta}{2\beta r_0 L + r^2 L + 2r^3 b_\theta}\right) + \frac{r^2L + 2r^3 b_\theta}{2\beta r_0 L + r^2 L + 2r^3 b_\theta}\chi_{pl}\right] 2\pi r_0 L S_p \\ &+ \frac{kT\pi r_0^2 L_t A_v}{2\phi \bar{V}_m^T}\left[\left(\frac{r}{r_0}\right)^2 + \left(\frac{r_0}{r}\right)^2 - 2\right] + \gamma_{sv} 2\pi(r - r_0)L_t - 2\pi r L\gamma_{lv}\cos\theta + 2\gamma_{lv}\pi r^2 a_\theta \ .\end{aligned} \tag{18}$$

Equation (18) is the governing equation for the cylindrical system. It is entirely defined by the geometric parameters L, r and r_0 and the state variables p and T.

3 Physical Implications

In the previous section we determined governing equations for the total free energy of both a spherical pore (16) and a cylindrical pore (18). In this section we examine the stability of liquid in a spherical pore and revisit results for the stability of liquid in a cylindrical pore from previous work [14]. With the wetting criteria for both spherical and cylindrical pores we can determine the effects of coupling such pores into a 'cluster-network' and also provide insight into the nature of long cylindrical water channels from more recent studies [13]. In our formulation we subtracted the constant free energy of a vapor filled pore $\mathcal{G}^0$, hence if $\mathcal{G} - \mathcal{G}^0$ is negative then liquid is favorable else vapor is favorable. After determining conditions for liquid stability we define a channel such that wetting occurs to determine the level in which the pore swells.

To compute the surface density of protons we assume $S_p = C\left(\bar{V}_m^T \cdot S\right)^{-1}$, where $\bar{V}_m^T$ is the specific molar volume of the membrane, S is the specific pore surface area, and C is a parameter we use to vary the value. We take the values, $\bar{V}_m^T = 537\, cm^3/mol$ and $S = 210\, m^2/cm^3$ for Nafion 117 from [16], and [18], respectively; with $C = 1$, $S_p = 8.87 \times 10^{-6}\, mol/m^2$. To compute $\mathcal{G} - \mathcal{G}^0$ we use a value of $\theta = 98^\circ$ taken from Zawodzinski et al. [27], which was measured at $p_r = 1$. Zawodzinski et al. finds that θ varies with water content; however, we are concerned with states near saturation therefore θ is held constant. For lack of a detailed data set we assign $\chi_{pl} = 0$ as in [28].

3.1 Pore Wetting

3.1.1 Unswollen Spherical Pores

We consider the case of spherical pores restricting the analysis to rigid pores, $r = r_0$, thereby investigating the size of the pore in which liquid fills the pore stably. The governing equation for the total free energy of a spherical pore system (16) for rigid pores yields

$$\mathcal{G} - \mathcal{G}^0 = \left[(p_{sat} - p) + \frac{R_w T}{v_l} \ln\left(\frac{X_l}{p_r}\right)\right] \frac{4}{3}\pi r_0^3 + R_u T \ln(1 - X_l)\, 4\pi r_0^2 S_p n + \left[(1-n) - n\cos\theta\right] \gamma_{lv} 4\pi r_0^2\,, \quad (19)$$

with

$$X_l = \frac{r_0}{r_0 + 3\beta n}\,. \quad (20)$$

Figure 3 shows (19) plotted against r_0 for values of surface coverage $n =$

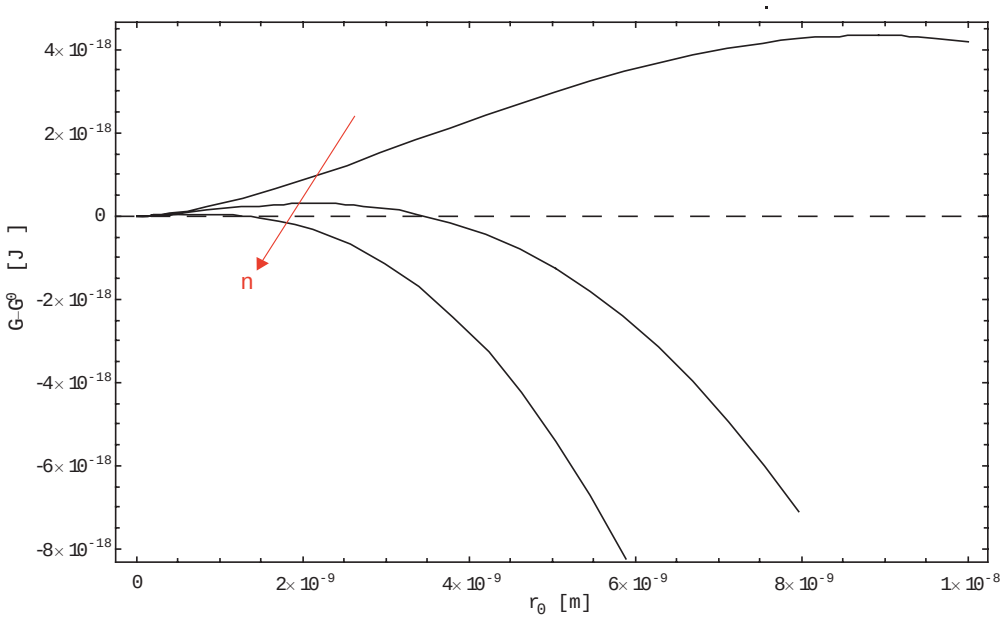

Fig. 3. Total Free Energy vs r_0 ($n = 0.4, 0.5, 0.6$) - Spherical Pore.

$0.4, 0.5, 0.6$. Recall that the surface coverage represents the ratio of solid-liquid interaction to the total area of the liquid droplet, whereas $1 - n$ represents the ratio of the pore that is open to channels, yielding a liquid-vapor interface for a liquid filled pore. Since r is restricted to r_0 this plot represents full pores of various sizes throughout the membrane, not pore growth. We see in the plot that as the surface coverage increases the critical radius for the stability of liquid decreases. These results may seem counter-intuitive at first glance, considering that Nafion is a hydrophobic surface; however, (19) stipulates that as we increase surface coverage (i.e. solid-liquid interface) we decrease liquid-vapor interface $(1 - n)$ proportionally. The factor $\cos\theta$ therefore means that an increase in the solid-liquid interface will have a lesser effect on the total free energy of the system than the corresponding decrease of the liquid-vapor interface. Increasing the surface coverage also increases the fraction of protons to water molecules that are in the mixture. In Figure 3 we see that for a fractional surface coverage of $n = 0.6$, liquid is stable in regions of radii larger than approximately $1.3\,nm$. If we decrease the surface coverage to $n = 0.5$, the stability criterion for liquid stability shifts to $3.4\,nm$ and even higher values for further decreasing coverage. Conversely, as the surface coverage goes to $n = 1$, i.e., no liquid-vapor interface at all, the critical radius is negligibly small ($0.75\,\mathring{A}$). We see again that at saturation ($p_r = 1$) the entropic desire for liquid dominates the hydrophobic repulsion of backbone surface. The inclusion of a liquid-vapor interface strongly impacts the system and we see that larger agglomerations are required for stability with decreasing surface coverage.

It is important to focus mainly on the trends in the plots as the values are sensitive to the parameters chosen, such as surface density of sulfonate sites

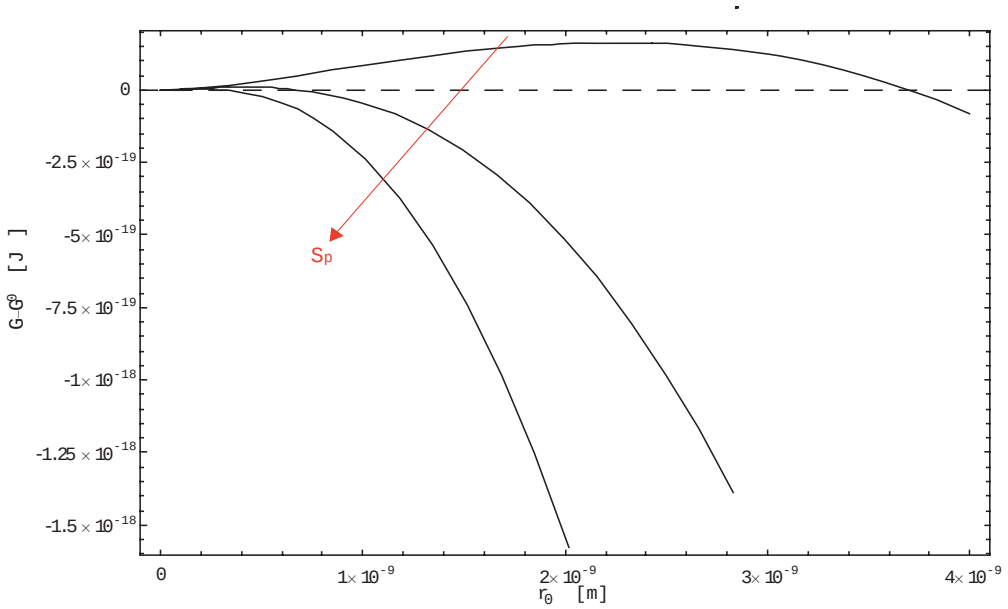

Fig. 4. Total Free energy vs r_0 ($\theta = 107°$ and $C = 1, 1/2, 1/4$) - Spherical Pore.

and contact angle of the backbone. The surface density of sulfonate sites was computed using the pore-specific surface value proposed by Divisek et al. using SPM methods [18]. In their calculation Divisek et al. assume the entire volume of micropores to be composed of pores with a radius of 1nm. Although differential curves of pore surface area seem to imply a sharp peak in the contributions to surface area centered around pores of radii of 1.5 nm, the value used for S_p can only be taken as an approximation if indeed the SPM method produces accurate results. The value of the contact angle θ can also only be considered an approximation. In the work by Zawodzinski et al., the contact angle of liquid water and Nafion was measured at the surface of the membrane where the properties may be dissimilar to those within the membrane. It has been proposed that the membrane may be covered with a nanoscopic hydrophobic 'skin' [27][12].

The effect of the parameters θ and S_p is shown in Figure 4. We show that stability criteria can change by plotting the free energy of a spherical pore of $n = 0.95$, with $\theta = 107°$ and $C = 1, 1/2, 1/4$. An increase in contact angle, and a decrease in sulfonate site density, dramatically increases the critical radius for the stability of the liquid phase.

3.1.2 Unswollen Cylindrical Pores

We recall briefly the results for rigid cylindrical pores [14], in order to examine the recent parallel pore model proposed by Schmidt-Rohr and Chen [13], and to examine the effect of the coupling of spherical and cylindrical pores.

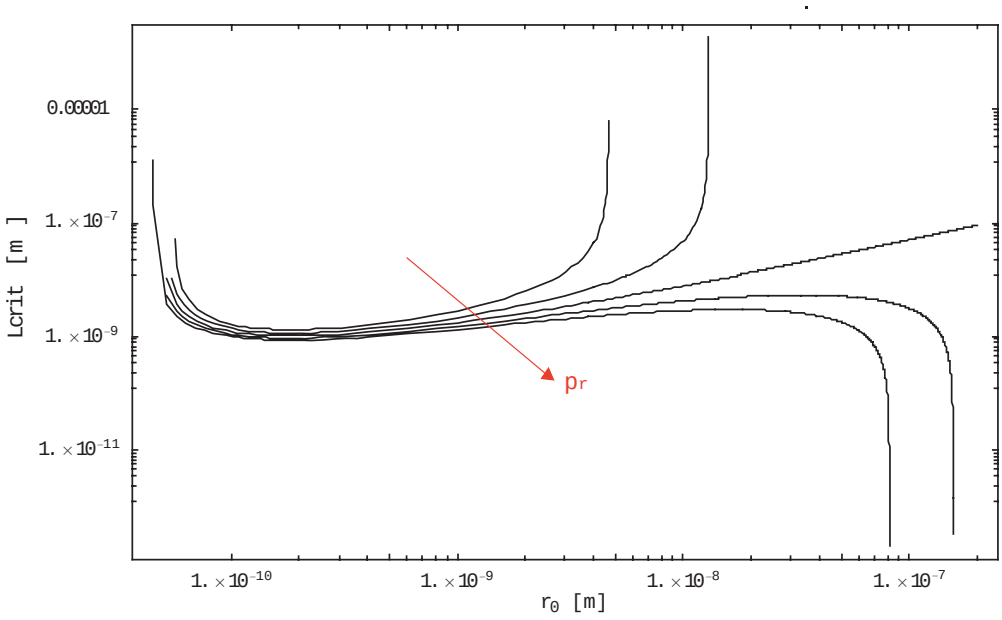

Fig. 5. Critical Length vs r_0 ($p_r = 0.8 : 1.2$) - Cylindrical Pore.

The critical length $L_{crit}(r)$ is obtained as the solution of $\mathcal{G} - \mathcal{G}^0 = 0$ from 18 with $r = r_0$. Figure 5 shows a log-log plot of $L_{crit}(r)$ for various pressure ratios p_r. The curves indicate that the stability of liquid depends on the level of saturation. The effects of the pressure ratio p_r are much stronger for wider pores, where the entropic effects begin to dominate. We see that in at saturation, $p_r = 1$, the change in L_{crit} with r_0 remains fairly linear. For under-saturated environments, $p_r < 1$, as pores become wider the critical length grows infinite making very wide pores totally unstable, regardless of length. In over-saturated environments, $p_r < 1$, the opposite is true, as pores become wider, L_{crit} becomes negligible, meaning the pores are stable for any length.

Schmidt-Rohr and Chen have estimated from SAXS data that the water channels in Nafion have an average radius of 1.2 nm [13]. We see in this theoretical analysis that pores of that size would be less susceptible to fluctuations in saturation than wider pores. Moreover the Schmidt-Rohr findings conclude that the persistent length of the pores is longer than expected, on the order of tens of nanometers, we see here that this analysis predicts that such a geometry would be very stable even with moderate under-saturation.

3.1.3 Cluster and Channel Configuration

The cluster-channel morphology introduced by Gierke et al. can be deconstructed into a network of the cylindrical and spherical pores discussed above. For a channel separating two clusters, the energetics of the clusters would be described as above with n equal to the ratio of the area of polymer interface

over the total area of the spherical region. From the dimensions for the Gierke cluster-network model, this would imply $n \approx 0.95$, and therefore liquid would be very favorable in saturated conditions. A channel between two liquid filled clusters is indeed equivalent to a cylindrical pore that is bounded by saturated liquid. From the analysis in [14], we know that in saturated liquid conditions a liquid filled channel is energetically very favorable in comparison to vapor filled. It is also interesting to note that, if the clusters were not liquid filled, the channel between the clusters ($L = 1\,nm$ and $r_0 = 0.5\,nm$) would not be filled with liquid as well (see Figure 5).

What we see then, in general, is that with the geometry described by Gierke et al., spherical pores (or clusters) will fill first, and if there is a cylindrical pore (channel) joining two clusters it will then proceed to fill. There is very little information available on the formation of channels between ionic clusters. Despite this, Ioselevich et al. insist the channels are required to explain the high protonic conductivity of Nafion as in the Gierke model [29]. They outline a methodology in which the formation of channels may be investigated using the minimization of free energy in [29], which is a similar strategy to the analysis employed in this work. We must note that while in the geometry of Gierke et al. the spherical pores are prerequisite to ensure the stable filling of channels, the cylindrical pores described by Schmidt-Rohr and Chen are stable independent of spherical pores.

4 Pore Swelling

In this section we prescribe an initial configuration, for a cylindrical pore and a spherical pore, such that the pore will be filled with liquid, according to the analysis in the previous section. We then allow the pore to swell past the initial radius in order to observe the effects of the deformation of the membrane on the total free energy of the system.

4.1 Cylindrical Pore Swelling

A full pore in Nafion may begin to swell in order to take on more water. The increase water content alters entropy of mixing and the swelling of the membrane increases the interfacial area thus increasing the surface free energy.

To compute the amount of swelling for a given pore we use the governing equation for the total free energy of a cylindrical pore system (18). We assume

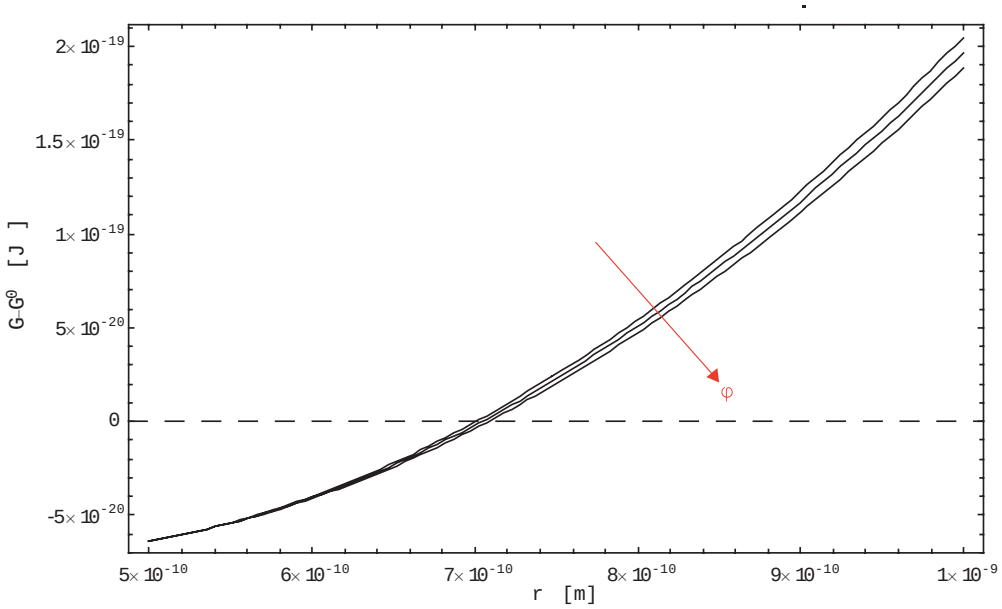

Fig. 6. Total Free Energy vs r ($\phi = 1/2, 1/3, 1/4$) - Cylindrical Pore ($r_0 = 0.5\,nm$, $L_t = 2\,nm$).

that the solid-vapor surface tension is negligibly small and accordingly set $\gamma_{sv} = 0$. We specify the geometry of the undeformed pore as $r_0 = 0.5nm$, and $L_t = 2\,nm$. Dimension similar to those proposed by Gierke et al. for their network channels. The length of the channel is such to ensure the stability of the liquid phase as indicated in Figure 5. The porosity of the membrane, ϕ, specifies the ratio of the undeformed pore size to the amount of membrane that it stretches as given by (7). Divisek gives a pore volume to membrane volume ratio of 0.38 for Nafion 117 in a saturated vapor environment, and up to 0.44 for Nafion 112 [18]. The value of porosity for Nafion 117 translates to $\lambda = 18.3$. indicating that some of the water is likely surface water; several values are used here for a lack of more comprehensive data.

In Figure 6 we plot the $\mathcal{G} - \mathcal{G}^0$ as a function of r for values of $\phi = 1/2, 1/3, 1/4$. We see that despite the liquid filled state being favorable, no swelling would occur, which is contrary to experimental evidence. The problem is that we specify that the channel will swell uniformly, which would cause the liquid-vapor interface to grow along with the channel radius. The liquid-vapor interface is a dominant contribution to the free energy and therefore the total free energy of the system grows when r is increased. In all likelihood, we presume, the channel would rather deform in an irregular fashion, keeping the liquid-vapor interface relatively constant.

To approximate non-uniform deformation, we restrict the liquid-vapor interface to r_0, while allowing the rest of the channel to deform to r. Figure 7 shows

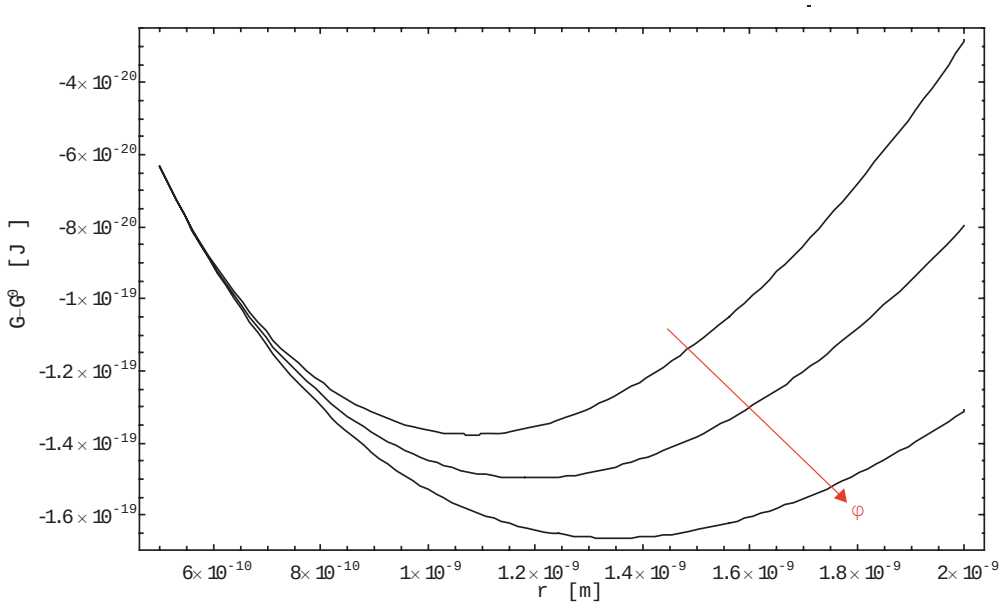

Fig. 7. Total Free Energy vs r ($\phi = 1/2, 1/3, 1/4$) - Cylindrical Pore ($r_0 = 0.5\,nm$, $L_t = 2\,nm$) with a constant liquid-vapor interface.

the total free energy of the cylindrical pore system with a constant liquid-vapor interface of radius r_0 over $r > r_0$ for values of porosity $\phi = 1/2, 1/3, 1/4$. The figure shows distinct minima of total free energy at values of $r > r_0$, and increasing with porosity. Increasing porosity implies an decrease in the effective amount of polymer that is deformed, accordingly the equilibrium radius of the swollen pore is increases. At a porosity of $1/2$ the pore is deforming to up to three times its radius, which would lead to a two-fold membrane deformation; at a porosity of $1/4$ the pore size doubles which would give a 125% growth of the entire membrane [1] .

Keeping the liquid-vapor interface constant is an idealization that is perhaps too great to yield accurate results. Nevertheless, we can see that the contribution of the liquid-vapor interface to total free energy is dominant enough to predict rather non-uniform swelling of a liquid filled cylindrical pore with such an interface. Equation (18) shows that the contribution of the liquid-vapor interface, to the total free energy of the system, does not depend on L_t and thus if the length of the liquid in the pore is very large (facilitated by a large L_t), compared to the radius of the liquid-vapor interface then the significance of the interface becomes marginal and we can then potentially see an increase in the liquid vapor interface.

[1] We relate pore volume to membrane volume using (7).

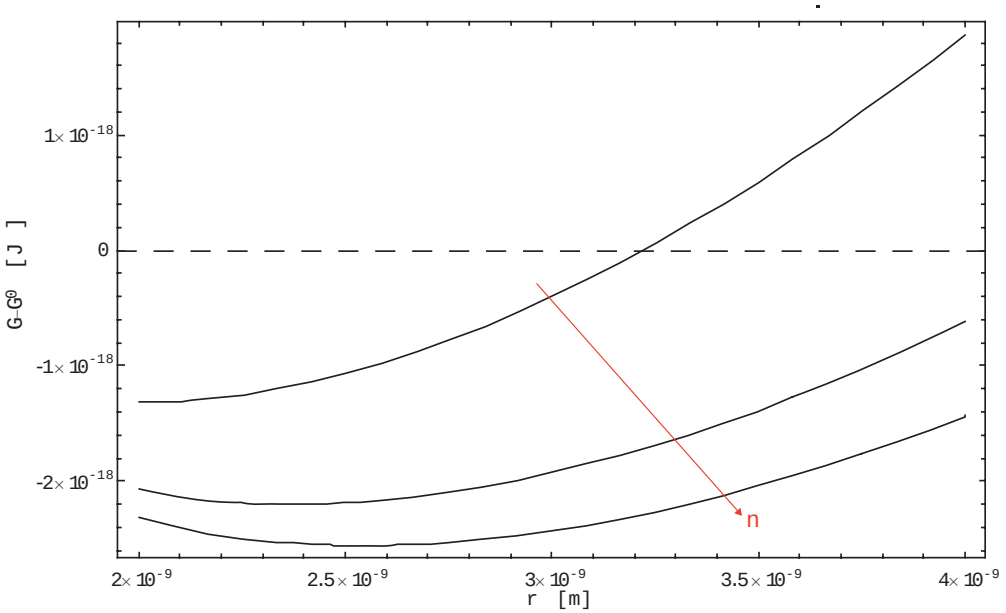

Fig. 8. Total Free Energy vs r ($n = 0.8, 0.95, 1$) - Spherical Pore ($r_0 = 0.5\,nm$).

4.2 Spherical Pore Swelling

We repeat the analysis for the swelling of a spherical pore. The constants specified above are again used, and the initial radius of the pore is set to $r_0 = 2\,nm$ which is the value set by Gierke and Hsu [3] [4]. In Figure 8 we study the swelling of a spherical pore swelling with $\phi = 0.25$ for values of $n = 0.8$, 0.95, 1. We see that no swelling occurs at lower values of the surface coverage parameter n, and increases with larger n. This, again, shows that the liquid-vapor interface plays a dominant role in swelling behavior.

For further study, we consider a fixed surface coverage of $n = 0.95$, so that the spherical pore has a large solid-liquid interface in comparison to the liquid-vapor interface. Figure 9 shows the total free energy of this pore for varying values of porosity $\phi = 1/2, 1/3, 1/4$. We see, again, that as the amount of polymer per pore decreases, and we observe an increase in the final equilibrium radius of the pore from $2.35\,nm - 2.6\,nm$, between $\phi = 1/4$ and $1/2$, respectively.

As in the cylindrical case, in an effort to simulate nonuniform swelling, we fix the liquid-vapor interface to be constant. The liquid-vapor interface is held at $(1 - n)\,4\pi r_0^2$, while the rest of the pore grows with r. Figure 10 shows a spherical pore swelling with $n = 0.95$ for values of $\phi = 1/2, 1/3, 1/4$; however, this time with the liquid-vapor interface constrained. We see somewhat more swelling with this modification, despite the small liquid-vapor interface with

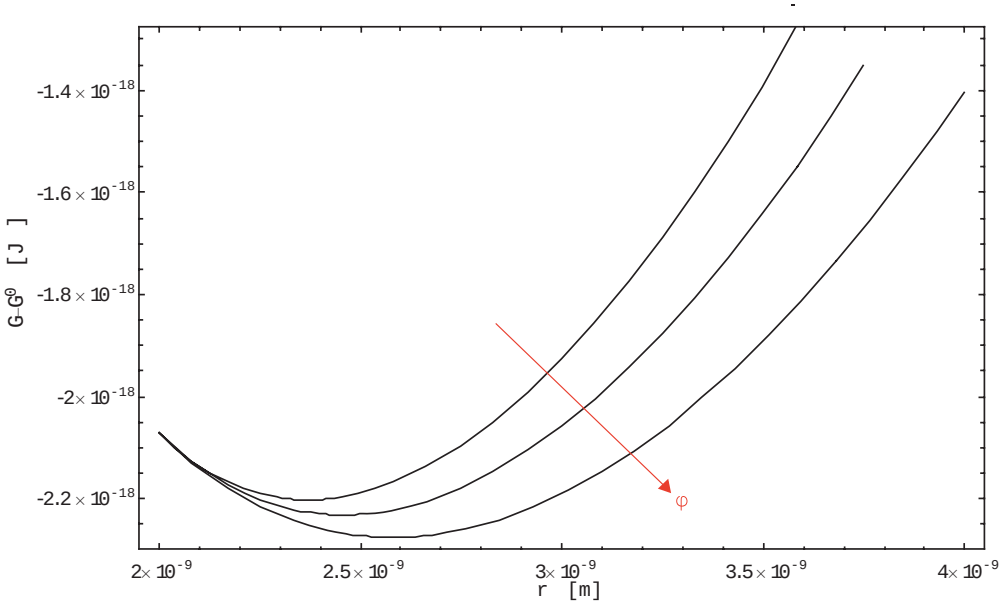

Fig. 9. Total Free Energy vs r ($\phi = 1/2, 1/3, 1/4$) - Spherical Pore ($r_0 = 0.5\,nm$).

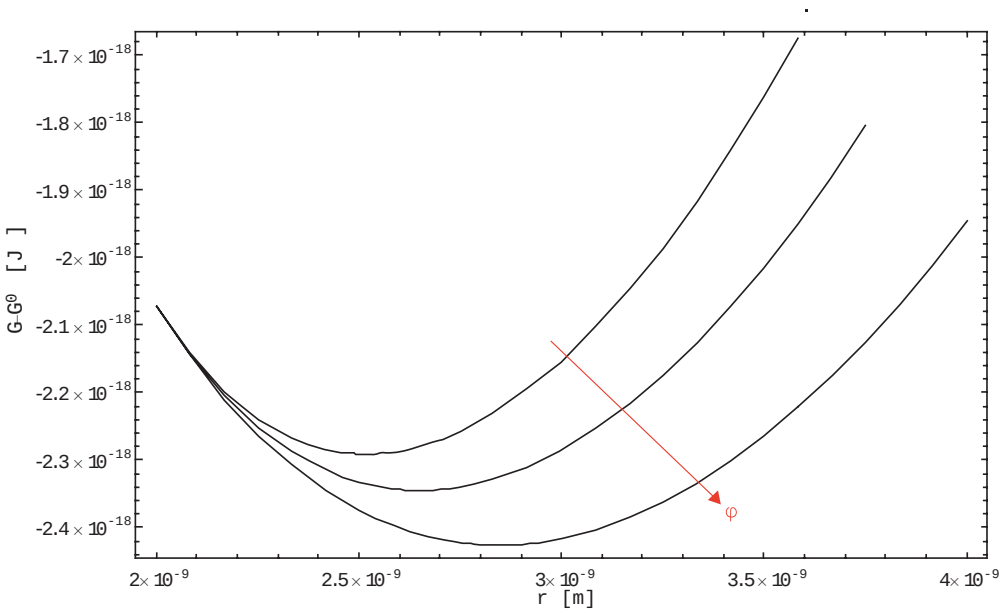

Fig. 10. Total Free Energy vs r ($\phi = 1/2, 1/3, 1/4$) - Spherical Pore ($r_0 = 0.5\,nm$) with a constant liquid-vapor interface.

$n = 0.95$ [2]. We see that the initial radius of $r_0 = 2\,nm$ swells to a radius between $2.5\,nm - 3\,nm$, depending on porosity.

In a similar analysis of the equilibrium size of spherical clusters of water in

[2] n is defined at r_0, since we are holding the liquid-vapor interface constant and allowing the pore to grow in r, n is effectively increasing as well.

Nafion [3] [4], Hsu and Gierke find that for Nafion 117, clusters of diameter $3.99\,nm$ should be observed in a saturated environment. Hsu and Gierke do not focus on regions which may support liquid wetting, instead their analysis presupposed uniform dry cluster sizes of $2\,nm$ throughout the membrane, which swell to $4\,nm$ in equilibrium with a saturated vapor. We find somewhat less swelling, with an equilibrium radius of not more than $3\,nm$ resulting from our analysis. Hsu and Gierke make the assumption that each cluster stretches an infinite and continuous elastic medium, which is defined by an empirical tensile modulus $G(c)$. Freger points out that approximating the polymer as a Hookean medium to yield an elastic energy for polymer is imprecise [24], we used here a change in free energy derived from the change in entropy of polymer chains as they are stretched [23]; this could explain some of the difference in the results.

5 Conclusions

The conductivity of a Nafion membrane has been shown to depend strongly on the amount of water sorbed. Experimental analysis of membranes has lacked sufficient detail to determine a conclusive morphological model of a Nafion membrane upon sorption. Since bulk water can be seen as the upper limit of protonic conductivity, it is important to determine the permeation of bulk-like water throughout the membrane in order to establish rigorous transport models.

We showed how the wetting of pores in a Nafion membrane is dictated by a competition of energetic and entropic forces. The energetic forces are due to the interfaces present, and accordingly scale with interfacial surface area. The entropic forces arise from mixing and the level of saturation; these forces scale with volume. Decreasing the surface density of sulfonate sites decreases the entropic desire for liquid water and increasing the hydrophobicity of the surface increases the energetic desire for vapor, both leading to an increase of the critical radius and critical length for the stability of liquid. The model shows that a cylindrical channel bounded by two water filled pores is very likely to sorb liquid water as this removes the liquid-vapor interfaces. The model also validates the stability of long thin channels proposed in recent studies.

Nafion is known to swell as it takes on water. To gain insight into this phenomenon we modeled the swelling of pores on the microscopic level. It was shown how, if present, a liquid-vapor interface is a dominant contribution to

the total free energy of the system, in particular for short pores. This leads to the conclusion that swelling at pore size level will be non-uniform.

Acknowledgment: This research was supported by the Natural Sciences and Engineering Research Council (NSERC).

6 List of Symbols

a_θ	end area function (1)
A	area (m^2)
A^U	unstretched area (m^2)
b_θ	end volume function (1)
g	specific Gibbs free energy (J/kg)
G	Gibbs free energy (J)
G_{el}	elastic free energy of membrane (J)
G_{mix}	Gibbs free energy of mixing (J)
$\mathcal{G}$	total Gibbs free energy of the system (J)
k	Boltzmann constant ($1.381 \times 10^{-23}\ J/K$)
L	length of liquid agglomeration (m)
L_t	length of pore (m)
m	mass (kg)
M	molar mass (kg/mol)
N	number of molecules
p	pressure (Pa)
p_r	pressure ratio (1)
p_{sat}	saturation pressure (Pa)
r	radius of liquid agglomeration (m)
$r_\circ$	unstretched pore radius (m)
R	specific gas constant ($J \cdot kg^{-1}K^{-1}$)
R_u	universal gas constant ($8.314\ J \cdot mol^{-1}K^{-1}$)
S_p	surface density of protons (m^{-2})
t	time (s)
T	temperature (K)
v	specific volume (m^3/kg)
V	volume (m^3)
X	mole fraction

Greek Symbols

α	volume ratio of stretched to unstretched pores
β	$S_p M_w/\rho_w$ (m^{-2})
γ	interfacial tension (J/m^2)
θ	contact angle ()
λ	water content ()
ν_e	effective number of chains in the polymer network ()
ρ	mass density (kg/m^3)
χ	interaction parameter ()

Subscripts

l	liquid
lv	liquid-vapor
m	membrane
p	proton
s	surface
sl	solid-liquid
sv	solid-vapor
v	vapor
w	water

Superscripts

0	unstretched vapor filled reference state

References

[1] K.A. Mauritz, R.B. Moore, State of Understanding of Nafion, Chem. Rev. 104 (2004) 4535-4585.

[2] T.D. Gierke, G.E. Munn, F.C. Wilson, The morphology in Nafion Perfluorinated Membrane Products, as Determined by Wide-Angle and Small-Angle X-ray

Studies, J. Polym. Sci., Polym. Phys. Ed. 19 (1981) 1687-1704.

[3] W.Y. Hsu, T.D. Gierke, Elastic Theory for Ionic Clustering in Perfluorinated Ionomers, 15 Macromolecules (1982) 101-105.

[4] T.D. Gierke, W.Y. Hsu, Ion-Transport and Clustering in Nafion Perfluorinated Membranes, J. Membr. Sci. 13 (1983) 307-326.

[5] M. Fujimura, T. Hashimoto, H. Kawai, Small-Angle X-Ray Scattering Study of Perfluorinated Ionomer Membranes 2. Origin of Scattering Maximum, Macromolecules 14 (1982) 1309-1315.

[6] M. Fujimura, T. Hashimoto, H. Kawai, Small-Angle X-Ray Scattering Study of Perfluorinated Ionomer Membranes 2. Models for Ionic Scattering Maximum, Macromolecules 15 (1982) 136-144.

[7] H.L. Yeager, A. Steck, Cation and Water Diffusion in Nafion Ion Exchange Membranes: Influence of Polymer Structure, J. Electroch. Soc. 128 (1981) 1880-1884.

[8] M.H. Litt, A reevaluation of Nafion Morphology, Polym. Prepr. 38 (1997) 80.

[9] H.G. Haubold, T. Vad, H. Jungbluth, P. Hiller, Nano structure of Nafion: a SAXS study, Electrochim. Acta 46 (2001) 1559-1563.

[10] B. Dreyfus, G. Gebel, P. Aldebert, M. Pineri, M. Escoubes, M. Thomas, Distribution of the micelles in hydrated perfluorinated ionomer membranes from SANS experiments, J. Phys. (France) 51 (1990) 1341.

[11] K.D. Kreuer, On the development of proton conducting polymer membranes for hydrogen and methanol fuels, J. Membr. Sci. 185 (2001) 29-39.

[12] R.S. Mclean, M. Doyle, B.B. Sauer, High-Resolution Imaging of Ionic Domains and Crystal Morphology in Ionomers using AFM Techniques, Macromolecules 33 (2000) 6541-6550.

[13] K Schmidt-Rohr, Q. Chen, Parallel cylindrical water nanochannels in Nafion fuel-cell membranes, Nature Materials 7 (2008) 75-83.

[14] G.J. Elfring, H. Struchtrup, Thermodynamic Considerations on the Stability of Water in Nafion, J. Membr. Sci. 297 (2007) 190-198.

[15] P. Choi, R. Datta, Sorption in Proton-Exchange Membranes: An Explanation of Schroeder's Paradox. J. Electrochem. Soc. 150 (2003) E601.

[16] P. Choi, N.H. Jalani, R. Datta, Thermodynamics and proton transport in Nafion - I. Membrane swelling, sorption, and ion-exchange equilibrium, J. Electrochem. Soc. 152 (2005) E84-E89.

[17] P. Futerko, I-Ming Hsing, Thermodynamics of Water Vapor Uptake in Perfluorosulfonic Acid Membranes, J. Electrochem. Soc. 146 (1999) 2049-2053.

[18] J. Divisek, M. Eikerling, V. Mazin, H. Schmitz, U. Stimming, Yu. M. Volfkovich, A Study of Capillary Porous Structure and Sorption Properites of Nafion Proton-Exchange Membranes Swollen in Water, J. Electrochem. Soc. 145 (1998) 2677-2683.

[19] J. Fimrite, H. Struchtrup, N. Djilali, Transport Phenomena in Polymer Electrolyte Membranes - I. Modeling Framework, J. Electroch. Soc. 152 (2005) A1804-A1814.

[20] M. Eikerling, A.A. Kornyshev, U. Stimming, Electrophysical Properties of Polymer Electrolyte Membranes: A Random Network Model, J. Phys. Chem. B 101 (1997) 10807-10820.

[21] Stephen J. Paddison, Reginald Paul, T.A. Zawodzinski Jr., A Statistical Mechanical Model of Proton and Water Transport in a Proton Exchange Membrane, J. Electrochem. Soc. 147 (2000) 617-626.

[22] I. Müller, Thermodynamics, Pitman, Boston, MA 1985.

[23] P.J. Flory, Principles of Polymer Chemistry, Cornell University Press, Ithaca and London 1953.

[24] V. Freger, Elastic energy in microscoically phase-separated swollen polymer networks, Polymer 43 (2002) 71-76.

[25] L. Rubatat, A.L. Rollet, G. Gebel, O. Diat, Evidence of Elongated Polymeric Aggregates in Nafion, Macromolecules 35 (2002) 4050-4055.

[26] S.A.Safran, Statistical Thermodynamics of Surfaces, Interfaces, and Membranes, Addison-Wesley, Reading, MA 1994.

[27] T.A. Zawodzinski Jr., S. Gottesfeld, S. Shoichet, T.J. McCarthy, The contact angle between water and the surface of perfluorosulphonic acid membranes, J. Appl. Electrochem., 23 (1993) 86-88.

[28] A. Bensberg, Swelling and shrinking of polyacid gels, Continuum Mech. Thermodyn. 9 (1997) 323-340.

[29] A.S. Ioselevich, A.A. Kornyshev, J.H.G. Steinke, Fine Morphology of Proton-Conducting Ionomers, J. Phys. Chem B 108 (2004) 11953-11963.

Reply to the Reviewers' comments on

Thermodynamics of Pore Wetting and Swelling in Nafion

by G.J. Elfring and H. Struchtrup

Journal of Membrane Science
Ref.: Ms. No. JMS-071039

- Please note references [13] to [23] and [24] to [27] from the initial manuscript have become [14] to [24] and [26] to [29] respectively, in the revised manuscript. All references are pertinent to the revised manuscript.

- Changes are referred to by page A and paragraph B as **pg. A pr. B**

General Changes:

- Reference to the recent Schmidt-Rohr and Chen publication has been added [14]
- Reference to the recent Rubatat et al. publication has been added [25]

Both reviewers raised important points and in particular **Reviewer 1** made a lengthy list of suggested changes that we feel has made the revised manuscript much more thorough; in particular, it has given us a chance to address the findings in the Schmidt-Rohr and Chen paper published in Nature Material this January after the initial manuscript was submitted. Below we address the points raised by both reviewers and list the changes made in the revised version in reference to those points.

Reviewer #1

- Reviewer 1 feels that the in the paper *the modeling effort relies on the Gierke model, which was state-of-the-art back in 1983. The main (major) revision needed is to address the current recognition (recent models by Rubitat and Schmidt-Rohr) that the ionic domains are anisotropic in nature and rather rod-like as opposed to isotropic spherical pores.*

Here we wish to emphasize that the paper is based on simple spherical and cylindrical geometric constructs which can be used to assemble and analyze the antiquated but still often used Gierke model but just as easily can analyze the thermodynamic stability of the parallel pore model suggested recently by Schmidt-Rohr. Indeed the revisions to this paper include such an analysis which shows that this model predicts that the Schmidt-Rohr cylindrical channels are thermodynamically rather favorable. We have revised the manuscript to include these details on **pg.2 pr.1, pg.13 pr.2, pg.14 pr.2, and pg.19 pr.3**.

- The reviewer states that: *the concept that large open pores exist in the membrane in dry conditions is unrealistic and does not agree with recent PAS studies of Nafion.*

We agree that the evolution from a dry membrane to near-saturated conditions is beyond the scope of this paper; we now state more specifically that we are only considering near-saturation equilibrium conditions for liquid filled pores on **pg.3, pr.1**.

- The reviewer states that: *It would have been nice to restate the main assumptions considered in the previous paper [ref 14] that lead to equation (3), which are: liquid agglomeration fills the pore radially, environment close to saturation, proton are incompressible and the total volume of the protons stays constant.*

We agree that some more of the more important details from [14] should be restated here in order to establish a more convenient independence of this particular work. We have revised the manuscript to include these details on **pg.4 pr.2**.

- The reviewer states that *Equation (3) in this paper (as a function of free energy of the membrane and surface free energy) is not in the same form as equation (36) in reference [14] (as a function of Helmholtz free energy of the membrane and surface Helmholtz free energy).* And asks *what considerations are different here?*

We have made this equation more compact by using the Gibbs free energy rather than the Helmholtz free energy but they are in fact the same equation.

- The reviewer states that: *For equation (5), can you briefly add the assumptions made by Flory in order to understand why Freger stated that the Flory swelling model may not be appropriate to Nafion. However, as you underline, the Flory model is not appropriate, but you still use it. Would it not be more reasonable to derive your work from the Freger swelling model? Nevertheless, is this treatment an over simplification based on what is known about Nafion morphology and properties?*

We have included the assumptions made by Flory to the revised manuscript. We also emphasize the reasons why Flory's model is an oversimplification, namely that the crystallinity of the Nafion provides effective crosslinks and there is evidence of the anisotropy of polymeric aggregates; but also, that there is no consensus method that provides an effective alternative. In particular Freger's model also suffers from these faults but has a nonphysical finite free energy of stretching at the rest state. Certainly we agree a comprehensive alternative to Flory's model for Nafion would certainly be welcome. The revisions to the manuscript are found on **pg.5 pr.3**.

- The reviewer states that: *Equation (7) states that the volume of membrane is linearly proportional to the volume of the pore. Do you have any references or experimental evidence that supports this conclusion? You are assuming a two phase model that Nafion is exclusively made of a perfluorinated backbone as the matrix and ionic aggregates as the pores. Is there ant contribution from more local free volume between chains?*

We use linear proportionality as a first estimate to establish the amount of membrane deformed by any particular pore for the purpose of analyzing swelling but we in fact study a range of values. We now state this fact more clearly and refer to the plots of changing porosity to describe how the change in membrane per pore affects the swelling. These changes in the manuscript are found on **pg.6 pr.2**.

- The reviewer states that we should *add the figure that was in paper [14] that shows the contact angle at the three phase points that supports Young's equation (12).*

This figure is now included on in **pg.3**.

- The reviewer states that: *It is difficult to follow the mathematical developments and geometrical arguments that lead to equations (15), (16), (17) and (18) from equations (5) and (8). Perhaps the authors could consider adding an appendix or "supplementary materials" that could contain the detailed derivation of the important equations. It helps to understand the assumptions made and how they affect the final formulas.*

Rather than add supplementary materials we've attempted to elaborate the geometric arguments to make the section less obfuscated. These changes in the manuscript are found on **pg.8 pr.1-2** and **pg.9 pr.1-2**.

- *Make sure the reader understands that when you talk about pore size, you also mean ionic aggregate size.*

Thanks for this note; a typo on **pg.10 pr.1** which caused an ambiguity has been corrected.

- *I am wondering if the contact angle taken into account really reflects the contact angle of water in very small channels. Surface contact angle and bulk contact angle may be different due to the geometry. The authors looked at the effect of a change in the contact angle and surface density of protons, but it would be interesting to see how the contact angle is affected by the size of the pores.*

Certainly the current experimental data leaves much to be desired. Measurements of the contact angle in Nafion would be most insightful; again, the uncertain nature of the contact angle, as you note, is why we studied the affects of its variation.

- *Figure 5 needs more explanation. I am not sure how that graph needs to be analyzed. Perhaps it would help to define the areas of stability/instability and the areas of under/over saturated environments.*

We've rewritten the explanation of Figure 5 on **pg.13 pr.1** to better define the regions which indicate stability and instability and over and under saturated environments.

- The reviewer states that: *The cluster and channel configuration paragraph clearly shows that the model developed is based on the morphology proposed by Gierke and also under one specific condition which is in saturated liquid conditions. The authors ignore the transient conditions that lead to a swollen membrane. The swelling process is composed of both sorption of vapor water and liquid water, or vapor water that then condenses to form liquid water. How does it affect the model? What if there is a structural evolution (where the geometry changes) as proposed by Gebel? This is again a more modern approach to that of Gierke.*

As mentioned above, we would like to point out that the model was developed not based on the Gierke morphology but with simpler geometric constructs; therefore, an analysis of the

Schmidt-Rohr parallel pore morphology can be done in the same manner, as shown on **pg.13 pr.2**.

- The reviewer states that: *The second paragraph (page 15) underlines the fact that the model for a cylindrical channel is valid if the channel is entirely filled with liquid water. Are there any conditions that could lead to an increase of a liquid vapor and solid vapor interfaces?*

If a change in pressure caused the liquid to become unstable then this would lead to evaporation. The liquid vapor interface is a large positive contribution to free energy therefore it would have to be negligible in magnitude such as for very long thin channels. These details are found on **pg.16 pr.2**.

- The reviewer states that: *According the last paragraphs, the reader may get to the conclusion that the swelling of Nafion membrane is mainly due to spherical pore swelling. Is it what the authors really want to say? Again, what if spherical clusters do not exist at all - just cylindrical channels as indicated with modern SAXS studies.*

The conclusions have been revised to put less emphasis on the spherical pores and to include reference to the long cylindrical pores put forward in the Schmidt-Rohr work. These details are found on **pg.19 pr.3**.

- The Reviewer concludes that *overall, this is an interesting and important field of study. With these detailed considerations of the thermodynamics it would be MOST valuable to the community to consider the state-of-the-art morphology, as opposed to an old model that is basically discounted.*

As described above we've included numerous references to the Schmidt-Rohr work published in January in Nature. We feel that this work anticipates their findings and shows how the long thin cylindrical channels are a very thermodynamically stable geometry.

Reviewer #2

- The reviewer states that: *The total Gibbs energy could be written with geometry depend free energy expressions.*

We're not certain if this comment was meant to *state geometry independent free energy expressions*; if so, we point out that before the geometric properties are applied, the derivation is done in a general fashion culminating in equation (13).

- The reviewer states that: *this paper adopted the old Flory's model, and there are some concerns regarding applying this approach in the Nafion system.*

As noted above we've included more details on the assumptions made by Flory and the concerns with its use for Nafion. These details are found on **pg.5 pr.1**.